Experimental Characterization of Material Properties to Simulate Needle Indentation Into Soft Tissues

Elizabeth Mesa-Múnera[a*], Juan F. Ramírez-Salazar[a], Pierre Boulanger[b] and John W. Branch[a]

[a]Department of Systems Engineering., National University of Colombia, Medellín, Colombia;
[b]Department of Computing Science, University of Alberta, Edmonton, Canada.

ABSTRACT

Surgical needle insertion has an important role in applications such as biopsies, neurosurgery and tumor ablation, and many studies have been carried out to simulate these types of procedures. The realistic simulation of tool-tissue interactions is required for the development of surgical simulators, and accurate biomechanical tissue models are determinant in their effectiveness. Previous works had characterized soft tissue properties; however, it is missing an appropriated validation of the results. In this paper, we used several hyperelastic models to replicate mechanical behavior of a silicone rubber under an indentation test. An uniaxial compression test was performed on the phantom tissue, with mechanical properties similar to brain, to estimate the parameters of the models using an optimization algorithm. The best fitted model is then used to validate the parameters in a FEM simulation of needle indentation comparing with experimental measurements. We found that the second order Reduced Polynomial model showed to be a good agreement for the material behavior (R-squared = 0.9922) and was stable for all strains. The simulation results of needle indentation using that material model gave us an R-squared error of 0.9613 with respect to the experimental values. Finally, we validated the used of an Optical Tracking system as a tool for measuring the position of the needle in real time. We compare those measures with the ones given by the stepper motor and we obtained an R-squared of 0.9999.

Keywords: Finite Element Method, soft tissue characterization, needle indentation

1 INTRODUCTION

Surgical simulators have been developed for a wide range of procedures and they can be classified into three main categories, needle-based, minimally invasive, and open surgery. Needle insertion is a well-known procedure due to its application in Minimally Invasive Surgeries (MIS), such as biopsies, brachytherapy, neurosurgery, and tumor ablation. Neurosurgical needle insertion is a type of MIS that is performed with a restricted field of view, displaced 2D visual feedback, and distorted haptic feedback. Much research and development have been devoted for training surgeons in MIS using visual and haptic feedback, but the accurate characterization of soft tissues for haptic simulation remains an open research area [1].

Considering the current development of real-time deformable models for surgery simulation, the techniques to acquire brain properties, and the integration of haptic feedback into surgical training interfaces, it is still necessary to implement experimental studies to measure mechanical properties of soft tissue and compare the results obtained with tool-tissue interaction models with empirical data. To obtain the most accurate results compared to the real ones, it is required to characterize soft tissue using *in-vivo* measurements. Some researchers have evaluated soft tissue properties *in-vivo*, *ex-vivo*, or in phantom tissue, using stretching tests [2], aspiration experiments [3], compression tests and, needle insertion for linear [4] and nonlinear biomechanical models [5]. In all these cases, researchers showed that their parameters correctly fit the experimental data used in the material calibration. However, there is only a few studies that evaluate the estimated material properties in different setups by comparing the results with additional experimental data.

We estimated the material parameters of a silicone rubber cube (with similar mechanical properties as brain matter) by performing a standard compression test in conjunction with an optimization algorithm. In addition, we validated the results using a Finite Element Method (FEM) simulation of a needle indentation, and compared the data with the corresponding force-displacement measurements. With this study we analyzed the feasibility of using an Optical Tracking System (OTS) for the development of a new *in-vivo* characterization device that measures (in

*Corresponding author. E-mail: emesamun@unal.edu.co.

real-time) the position of the needle. This analysis was done using the displacement data from an stepper motor as a reference and comparing the measurements with the ones from the OTS. The obtained material model can be used for subsequent surgical simulations that include haptic feedback during the indentation of a needle into a virtual brain.

2 THEORETICAL FOUNDATIONS

2.1 Hyperelasticity

Different constitutive laws are used to model the mechanical response of a material according to its behavior [6]. These models are obtained by fitting experimental measurements to a set of equations that relate stresses and strains, and they must satisfy the laws of thermodynamics. These constitutive laws apply for materials that show an elastic behavior under very large strains. Hyperelastic models are required when the material is subjected to finite displacements, whereas elastic theory is restricted to infinitesimal displacements. Hyperelasticity constitutes the basis for more complex material models, including phenomena such as viscoelasticity and tissue damage. The general form of the constitutive equation for a hyperelastic material in terms of the Strain Energy Density Function W, the Deformation Gradient Tensor F, the Cauchy Stress Tensor σ_{ij}, and the Jacobian J of the deformation gradient is given by Eq. 1.

$$\sigma_{ij} = \frac{1}{J} F_{ik} \frac{\partial W}{\partial F_{kj}}, \tag{1}$$

Depending on the complexity of W, different features such as nonlinearity and anisotropy can be included into the model. The most representative forms of W (usually included in commercial FEM software and considered in this study) with their correspondent definitions of initial shear modulus μ are shown in Eq. 2.

$$\begin{aligned}
&\text{Neo-Hookean:} && W = C_{10}(\bar{I}_1 - 3) + \frac{K_1}{2}(J-1)^2, && \mu = 2C_{10}. \\
&2^{nd}\text{ Order Reduced Pol.:} && W = \sum_{i=1}^{N} C_{i0}(\bar{I}_1 - 3)^i + \sum_{i=1}^{N} \frac{K_i}{2}(J-1)^{2i}, && \mu = 2C_{10}. \\
&\text{Mooney-Rivlin Solid:} && W = C_{10}(\bar{I}_1 - 3) + C_{01}(\bar{I}_2 - 3) + \frac{K_1}{2}(J-1)^2, && \mu = 2(C_{10} + C_{01}). \\
&\text{Ogden Form:} && W = \sum_{i=1}^{N} \frac{2\mu_i}{\alpha_i^2}(\bar{\lambda}_1^{\alpha_i} + \bar{\lambda}_2^{\alpha_i} + \bar{\lambda}_3^{\alpha_i} - 3) + \sum_{i=1}^{N} \frac{K_i}{2}(J-1)^{2i}, && \mu = \sum_{i=1}^{N} u_i,
\end{aligned} \tag{2}$$

where, C_{i0} and K_i are temperature-dependent material parameters, the bulk modulus K is equal to K_1 for all models, and W can be defined in terms of the invariants (I_1, I_2, I_3) of the Left Cauchy Green Deformation Tensor (B), the alternative invariants $(\bar{I}_1, \bar{I}_2, J)$ of B, or in terms of the principal stretches $(\lambda_1, \lambda_2, \lambda_3)$. Soft biological tissues can be approximated as nearly incompressible materials based on their high water content. To model this approximation, one simply sets the last term to zero. This is because $J = 1$ in the case of fully incompressible materials.

2.2 Uniaxial compression test: Analytical Solution

In the uniaxial compression test, the material is submitted only to normal stresses because the contact surfaces between the plates and the material are lubricated. Let us also assume an incompressible, homogeneous, isotropic material; therefore the transverse strains (perpendicular to the applied load) are considered to be the same, and the Poisson's ratio (ν) is 0.5. Using the constitutive equations (see Eq. 1 and 2), the analytical solution is given by Eq. 3 in terms of the Nominal Stress (S_{11}) and the principal stretches (λ_1) in the direction of the compression.

$$\begin{aligned}
&\text{Neo-Hookean:} && S_{11} = 2C_{10}(\lambda_1 - \lambda_1^{-2}), \\
&2^{nd}\text{ Order Reduced Pol.:} && S_{11} = 2(\lambda_1 - \lambda_1^{-2})(C_{10} + 2C_{20}(\bar{I}_1 - 3)), \\
&\text{Mooney-Rivlin Solid:} && S_{11} = 2(1 - \lambda_1^{-3})(C_{10}\lambda_1 + C_{01}), \\
&\text{Ogden Form:} && S_{11} = 2\frac{\mu_1}{\alpha_1}(\lambda_1^{\alpha_1 - 1} - \lambda_1^{-0.5\alpha_1 - 1}).
\end{aligned} \tag{3}$$

3 METHODS

As shown by Francheschini et al. [7], human brain tissue deforms similar to filled elastomers, and it should be modeled as a nonlinear solid with small volumetric compressibility. Girnary [8] also highlight that silicone brain phantoms provide good results to simulate brain behavior. We used a tissue phantom rather than biological tissue because this facilitates obtaining repeatable results in a controlled environment. Each component of the rubber

solution was evenly mixed according to the recommendations of the manufacturer and then formed in a box mold of $70 \times 80 \times 80$ *mm*. We used a force/torque sensor, (ATI Mini40 SI-40-2) with 0.02 *N* resolution, attached to a laparoscopic grasping tool, which was fixed to a rigid plate (see Fig. 1(a)). The plate was displaced using a stepper motor to compress the tissue at a constant velocity of 0.4 mm/s, until the plate was displaced by 12.7 *mm*. The contact areas were lubricated with talcum powder in order to minimize lateral friction. The grasping tool, the plate, and the phantom tissue had 3 *mm* diameter markers to record their 3D position during the complete test, at a frame rate of 100 *Hz*, using a commercial Optical Tracking System (OTS) from NaturalPoint.

We assumed the experiment occurs under symmetric conditions, with an homogenous, isotropic and incompressible material, and that imposed deformations were small compared with the original size of the block. The experimental Nominal Stress S_{11} was found by dividing the reaction force at every sample point by the undeformed contact area. The Nominal Strain corresponded to the displacement of the plate divided by the undeformed height of the block. We selected the hyperelastic models shown in Eq. 2 to estimate the mechanical response of our specimen. To calibrate the material parameters, we minimized the error between the stress-strain curve obtained with the analytical solution with respect to the experimental measurements. This estimation is performed using a least-square fit. We used absolute errors because they gave better fit for large strains (see Eq. 4). However, we also obtained the parameters by minimizing the relative error (the one used in ABAQUS) by fitting the solution to the experimental measurements that corresponded to deformations bigger than 0.05 (see Eq. 5).

$$\text{minimize}\{\text{Absolute Error}^2\} = \min\{\sum(S_{exp.} - S_{analytical})^2\}, \tag{4}$$

$$\text{minimize}\{\text{Relative Error}^2\} = \min\{\sum(1 - (S_{analytical}/S_{exp.}))^2\}, \tag{5}$$

Even if the founded parameters show a good fit in respect to the experimental data, it is required to study the stability of the material properties using the Drucker stability criterion, i.e. the material should satisfy the fundamental assumptions underlying continuum constitutive equations [6]. Once we selected the model that better fitted the experimental data, a FEM simulation of needle indentation was done in ABAQUS, and we compared the results with experimental measurements (Fig. 1(b)). The mesh size was graded to be more refined close to the indenter and coarse near the model boundaries. We allowed nonlinearities for the material model and large geometric deformations. Instead of simulating an indentor (which would required a contact interaction) we enforced displacement on nodes contained in the area where the needle was indented. The constrained nodes were located in a circular area of 5 *mm* diameter which was displaced at the same velocity than the compression test until the deformation was 10*mm*. Finally, we compared the measurements of the needle displacement using the OTS and the stepper motor to study the feasibility of work with an OTS for *in-vivo* characterization.

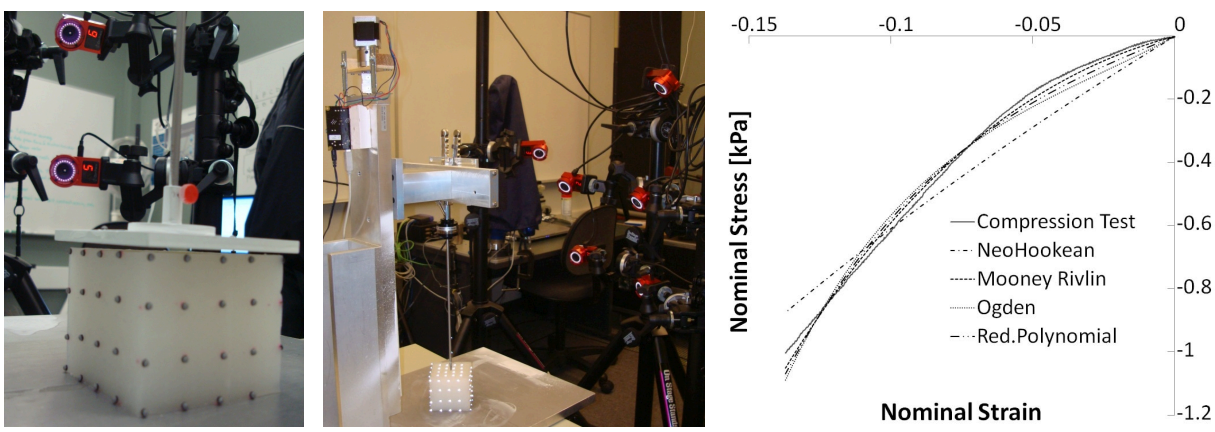

(a) Setup: Compression Test (b) Setup: Indentation (c) Results for Compression Test

Figure 1. Experimental setups and results for the material calibration.

4 RESULTS

After fitting the parameters we evaluated the goodness of fit using as the statistical measure the R-Square value (see Table 1). Results showed that material properties obtained with the minimization of the absolute error gave better fit than those obtained with relative errors. The Ducker Stability Check showed that the models were stable for all strains, except for the Mooney Rivlin model that has negative C_{10} parameter and was stable just for small strains ($\varepsilon < 0.05$). Even if the Mooney Rivlin model showed the best fit in respect to the experimental measurements,

the coefficients did not reflect the physics of the data and therefore are useless. Fig. 1(c) shows the results for the uniaxial compression test and the predicted stress-strain curves using different hyperelastic models obtained with the minimization of the absolute error.

Table 1. The R-squares value for each of the material models using absolute and relative error. The optimization using relative error was done considering large deformations ($\varepsilon > 0.05$).

Material Model	**Error**	**R-Squared**
Mooney Rivlin	Absolute	0.9969
Mooney Rivlin	Relative	0.9958
Reduced Polynomial (N=2)	Absolute	0.9922
Reduced Polynomial (N=2)	Relative	0.9900
Ogden Form	Absolute	0.9847
Ogden Form	Relative	0.9812
Neo-Hookean	Absolute	0.9386
Neo-Hookean	Relative	0.8941

We picked the Reduced Polynomial model (obtained minimizing the absolute error) to simulate the indentation using the following parameters: $C_{10} = 600.553\ Pa$ and $C_{20} = 4097.45\ Pa$. As one can see in Fig. 2(a)), where we present the deformable body after the needle was indented during the FEM simulation, we modeled just one quarter of the block because we applied symmetry boundary conditions. We also fixed the nodes that were located in the bottom of the box to imitate the experimental conditions. The R-squared value that compares the indentation simulation and the experimental measurements is 0.9613 and the differences of the force-displacement curves can be observed in Fig. 2(b).

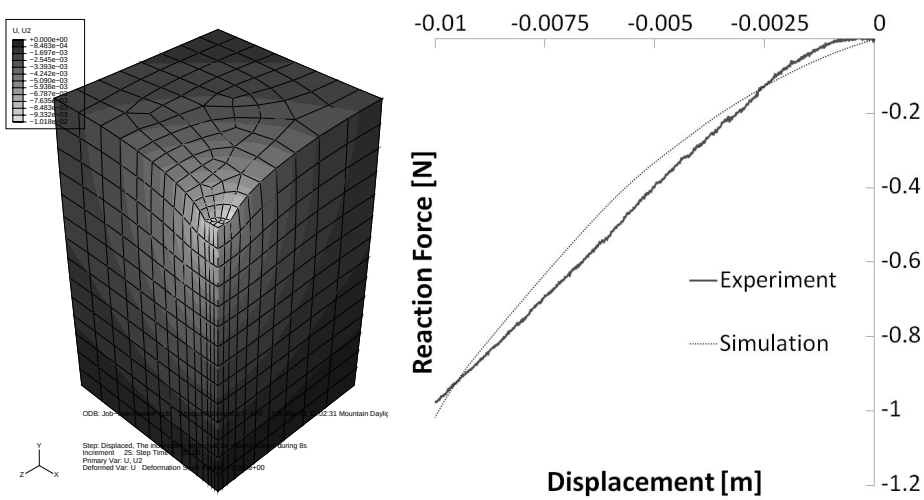

(a) FEM Simulation (b) Stress-Strain curve for indentation

Figure 2. Comparison of Simulation and Experimental Results

To evaluate the adequacy of using the OTS to measure the position of the needle in real-time, we measured independently the displacement of two markers that were located in the needle. If the OTS obtained perfect results, the displacement-time curve should be linear with pendent equal to the velocity that the needle was indented. As shown in Fig. 3, the results for both spheres were very closed, and the accuracy in terms of the R-squared values was 0.9999 and 0.9997, respectively.

5 CONCLUSION

This paper presents an approach for estimating hyperelastic parameters of soft tissue based on a simple compression test and using least-squares optimization. Those parameters were used in a FEM indentation simulation and the

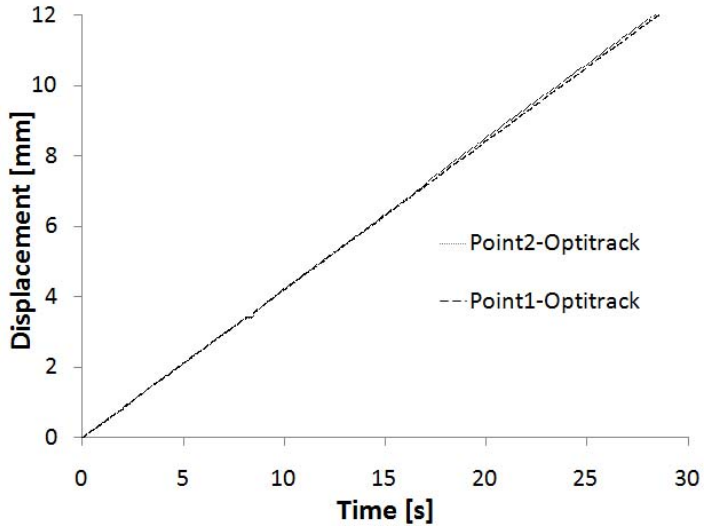

Figure 3. Optical Tracking Measurements for two different points located in the needle.

results were validated with experimental data. The material model that better fit the experimental data and was stable for all strains was the Second Order Reduced Polynomial Model. The results of the approximation using this material model corresponded to R-squares values of 0.9922 and 0.9613 for compression and indentation, respectively. The simulation results show acceptable prediction of forces and displacements, indicating that the method works well. We also demonstrated that the needle can be successfully tracked using the OTS for this type of experiments. Future work will explore the 3D geometrical deformation of the tissue, using the OTS, as an additional alternative to validate the results. We will explore more complex scenarios for indentation but using viscoelastic properties, different geometries, and in-vivo measurements.

References

[1] N. Abolhassani, R. Patel, and M. Moallem, "Needle insertion into soft tissue: A survey," *Medical engineering & physics* **29**(4), pp. 413–431, 2007.

[2] I. Brouwer, J. Ustin, L. Bentiey, A. Dhruv, and F. Tendick, "Measuring In Vivo Animal Soft Tissue Properties for Haptic Modeling in Surgical Simulation," *Medicine meets virtual reality 2001* , p. 69, 2001.

[3] M. Kauer, V. Vuskovic, J. Dual, G. Szekely, and M. Bajka, "Inverse finite element characterization of soft tissues," *Medical Image Analysis* **6**(3), pp. 275–287, 2002.

[4] S. DiMaio and S. Salcudean, "Needle insertion modeling and simulation," *IEEE Transactions on robotics and automation* **19**(5), pp. 864–873, 2003.

[5] J. Kim and M. Srinivasan, "Characterization of viscoelastic soft tissue properties from in vivo animal experiments and inverse FE parameter estimation," *MICCAI 2005* , pp. 599–606, 2005.

[6] A. Bower, *Applied mechanics of solids*, CRC, 2009.

[7] G. Franceschini, D. Bigoni, P. Regitnig, and G. Holzapfel, "Brain tissue deforms similarly to filled elastomers and follows consolidation theory," *Journal of the Mechanics and Physics of Solids* **54**(12), pp. 2592–2620, 2006.

[8] H. Girnary, "Brain Phantom Project," Master's thesis, Cornell University, 2007.